

First measurements of CFC-12 in 1951 at Jungfraujoch and comparison to current measurements and atmospheric models

Jamal Makkor¹, Mathias Palm², Irene Pardo Cantos³, Matthias Buschmann⁴, Emmanuel Mahieu³, Zihao WANG⁵, Martyn P. Chipperfield⁵, and Justus Notholt⁴

¹Universität Bremen

²University of Bremen

³University of Liège

⁴Institute of Environmental Physics, University of Bremen

⁵University of Leeds

June 26, 2025

Abstract

We prove results on unique continuation at the boundary for the solutions of real analytic elliptic partial differential equations of the form

$$\sum_{i,j=1}^n a_{ij}(x) \frac{\partial^2 u}{\partial x_i \partial x_j} + \sum_{k=1}^n b_k(x) \frac{\partial u}{\partial x_k} + c(x)u = 0$$

This work is motivated by and generalized the main results of , (missing citation), (missing citation), X.Huang et al in , (missing citation), (missing citation) and M.S Baouendi and L.P. Rothschild in (missing citation) Key words: Elliptic partial differential equation ; Hopf Lemma ; Unique continuation principle ; Real analytic hypersurface ; Real analytic functions

Hosted file

Makkor-AGU_Manuscript_v1.docx available at <https://authorea.com/users/934718/articles/1305178-first-measurements-of-cfc-12-in-1951-at-jungfraujoch-and-comparison-to-current-measurements-and-atmospheric-models>

References

22 Abstract

23 Chlorofluorocarbons (CFCs) have played a major role in the depletion of the stratospheric ozone
24 layer. Understanding the historical trend of emissions and atmospheric concentrations is crucial
25 for quantifying their environmental impact. The first direct measurements of atmospheric CFCs
26 were performed *in-situ* by Lovelock in 1970. We have analysed historical solar absorption
27 infrared spectra from 1951, recorded at the high Alpine Jungfrauoch site to retrieve the CFC-12
28 surface mole fraction. The results are compared to routine solar absorption measurements at
29 the site starting in 1984 and emission-based forward models. The surface value from the
30 historical spectra is 26.1 ± 18.5 ppt. This measurement agrees with model results within the
31 error bars although the model values may be biased low due to unreported emissions. Our
32 result represents the earliest atmospheric CFC measurement, predating Lovelock's detection by
33 over two decades.

34 Plain Language Summary

35 This paper presents the first worldwide measurement of CFC-12 surface mole fraction obtained
36 at Jungfrauoch in 1951. The study was performed using digitized paper-based solar spectra
37 produced by a Pfund-type grating spectrometer. The surface mole fraction was calculated using
38 modern retrieval methods, and compared with model predictions.

39 An analysis of errors is presented and compared with the reconstructed histories and AGAGE
40 models. The comparison gives a concentration three times higher than the one predicted by the
41 model. However, the model result and the reconstructed histories lie within uncertainty of
42 measurement.

43 1 Introduction

44 The compound CCl_2F_2 , more commonly referred to as CFC-12 or Freon-12™, was first
45 synthesised by Thomas Midgley ([Midgley & Henne, 1930](#)) and is one of the most important
46 atmospheric ozone-depleting substances (ODSs) regulated by the Montreal Protocol. It has an
47 ozone depletion potential (ODP) of 1.0 and contributes around 1000pptv of current
48 stratospheric chlorine loading ((WMO) Scientific Assessment of Ozone Depletion, [2022](#)). It is
49 also a potent greenhouse gas (GHG) with a Global Warming Potential (GWP) relative to CO_2 of
50 10900 over a 100-year horizon, one of the highest of the regulated gases (The Kigali
51 Amendment, [2016](#)).

52 CFC-12 was used for many decades due to its chemical non-reactivity and stability as a
53 refrigerant and as a propellant. Most of the reported production and emissions of CFC-12 (and
54 other regulated ODS) were reported by the Chemical Manufacturers Association ([CMA, 1980](#)).
55 In 2016, the global emissions of CFC-12 were estimated to be approximately 33 ± 21 Gg yr^{-1} ,
56 while in 2020, these emissions were estimated to have reduced to around 25 ± 20 Gg yr^{-1}
57 ((WMO) Scientific Assessment of Ozone Depletion, [2022](#)).

58 In July and August of 1970, James Lovelock discovered trace amounts of a similar
59 chlorofluorocarbon, CFCl_3 (CFC-11) and SF_6 , using a new and very sensitive Electron Capture
60 Detector (ECD) device when studying tropospheric haze over Ireland. Lovelock also tried to
61 measure CFC-12 in the atmosphere. However, this was not possible due to its relatively low rate

62 of reaction with thermal electrons in the electron capture detector ([Lovelock, 1971](#)). Later,
63 [Molina & Rowland, \(1974\)](#) proposed that CFCs would dissociate in the stratosphere when
64 exposed to ultraviolet radiation, freeing chlorine, and causing a catalytic reaction cycle that
65 destroys stratospheric ozone. This discovery was one prime motivation for the Montreal
66 Protocol (MP), which proposed a gradual phase-out of these gases (United Nations Treaty
67 Collection, [1989](#)). The Atmospheric Lifetime Experiment (ALE) started measuring multiple gases
68 including CFC-11 and CFC-12 in 1978 based on theoretical work of [Cunnold et al., \(1978\)](#) using
69 ECD-based chromatographs.

70 Following a continued increase in its atmospheric abundance, the first slowing in the
71 growth rate of CFC-12 was reported by [Engel et al., \(1998\)](#) based on *in-situ* balloon
72 measurements. The subsequent global decline in CFC-12, albeit slow due to the relatively long
73 lifetime of CFC-12 of more than 100 years, has contributed to the slow recovery of the ozone
74 layer ((WMO) Scientific Assessment of Ozone Depletion, [2022](#)). This global picture of declining
75 emissions of the major CFCs suffered a setback due to non-compliant production of CFC-11
76 from 2012, which was reported by [Montzka et al., \(2018\)](#) and later confirmed using FTIR
77 observations at Jungfraujoch and Lauder ([Cantos et al., 2022](#)). However, CFC-11 emissions now
78 seem to have returned to values consistent with expectations ([Montzka et al., 2021](#)).

79 In this work, we present the retrieval of CFC-12 from historical solar infrared absorption
80 spectra from a Pfund-type grating spectrometer together with FTIR spectra from both a home-
81 made (since 1984) and a commercial instrument (Bruker, since the 1990s) from the
82 International Scientific Station at Jungfraujoch, as well as an estimation of the surface
83 concentration of this gas. The retrieved CFC-12 values are compared to reconstructed histories
84 estimation of CFC-12 in 1951 as well as the AGAGE 12-Box Model ([Rigby et al., 2013](#)). The
85 digitization and calibration of the historical spectra has been published by [Makkor et al., \(2024\)](#).

86 **2 Materials and Methods**

87 **2.1 Retrieval theory**

88 The inverse model follows the optimal estimation or Tikhonov regularization formalism
89 proposed by [Rodgers, \(2000\)](#). It is a semi-empirical method of inverse calculation of the state of
90 the atmosphere. The optimal estimation method (following Bayesian statistics) constricts the
91 unknown state of the atmosphere to an *a priori* state vector x_a ,

$$\hat{x} = x_a + A(x_t - x_a) + \epsilon$$

92 Where \hat{x} represents the retrieved state, x_t is the true state of the atmosphere and A represents
93 the averaging kernels matrix, which provides an assessment of the sensitivity of the retrieval
94 over a given altitude range for a smooth profile. The retrieval requires an *a priori* profile that is
95 usually constructed to represent the general state of the atmosphere (layers, temperature,
96 pressure and gas profiles). The tool used to perform the retrievals is SFIT4 v1.0.21 developed by
97 the University of Colorado, Boulder, and maintained by the University of Bremen, Germany. It is
98 often used within the solar absorption infrared community of the Network for the Detection of
99 Atmospheric Composition Change (NDACC; [ndacc.org](#)).

100

101 2.1.1 The Spectroscopy

102 The line-by-line and pseudoline lists adopted in this work were provided by the AMT20
103 (additional missing lines can be compiled from <https://mark4sun.jpl.nasa.gov/pseudo.html>),
104 where for each gas, the line position, the strength and other parameters are compiled into a
105 line list that is then used to calculate the simulated spectrum based on radiative transfer
106 theory. In this work CFC-12 from the historical spectra is retrieved from the micro window 1
107 (MW1) [920.1-923.6 cm^{-1}] and the FTIR spectra from both the aforementioned and the micro
108 window 2 (MW2) [1160-1163 cm^{-1}] ([Mahieu et al., 2008](#)).

109 2.1.2 Instrumental parameters

110 The instrumental line shape (ILS) function used for the grating spectrometer can be described
111 by a sinc^2 function. SFIT4 requires the ILS in the interferogram domain. A sinc^2 function in the
112 spectral domain corresponds to a triangular apodization in the interferogram domain ([Griffiths,
113 2006](#)). It causes an artificial line widening and reduction in intensity. The overall resolution of
114 the Pfund-type grating spectrometer is usually between 0.1 and 0.4 cm^{-1} depending on the
115 wavenumber range and the grating used. However, in the retrieval, it must be considered that
116 the resolution of a grating spectrometer is wavelength dependent. The FTIR spectra from
117 Jungfraujoch are usually much lower in noise and higher in resolution than the grating-based
118 ones. The apodization function used during the retrieval is a boxcar function. The resolution is
119 0.012 cm^{-1} (OPD of 82 cm) for the home-made spectrometer and 0.008 cm^{-1} (OPD of 120 cm)
120 for the Bruker FTS-120HR.

121 The pressure, temperature and a priori water vapour profiles are obtained from the National
122 Centers for Environmental Prediction reanalysis (NCEP; [Kalnay et al., 1996](#)) and are extended
123 above 55 km using data from the Whole Atmosphere Community Climate Model version 7
124 (WACCMv7).

125 **3 Atmospheric Measurements at Jungfraujoch and models used**

126 3.1 Atmospheric measurements at Jungfraujoch

127 3.1.1 Grating measurements at Jungfraujoch

128 In 1949, Professor Migeotte and his team built and used a Pfund-type infrared grating
129 spectrometer with a 1-metre focal length, which was equipped with a PerkinElmer thermopile
130 detector, to record the solar spectrum at Jungfraujoch (46.55°N, 7.98°E, 3.58 km above sea
131 level) ([Migeotte, 1949](#)). The recorded spectra were saved on paper rolls using an electronically
132 guided pen. Altogether, these paper spectra covered a wavenumber range from 421 to 3571
133 cm^{-1} and contained handwritten atmospheric metadata such as surface temperature and
134 humidity ([Migeotte et al., 1956](#)). Spectra from 1951 have been scanned, digitized and calibrated
135 to the proper wavenumber range, and saved in a machine readable format ([Makkor et al.,
136 2024](#)). An example of the resulting digitized spectrum covering the retrieved region is shown in
137 [Figure 1](#).

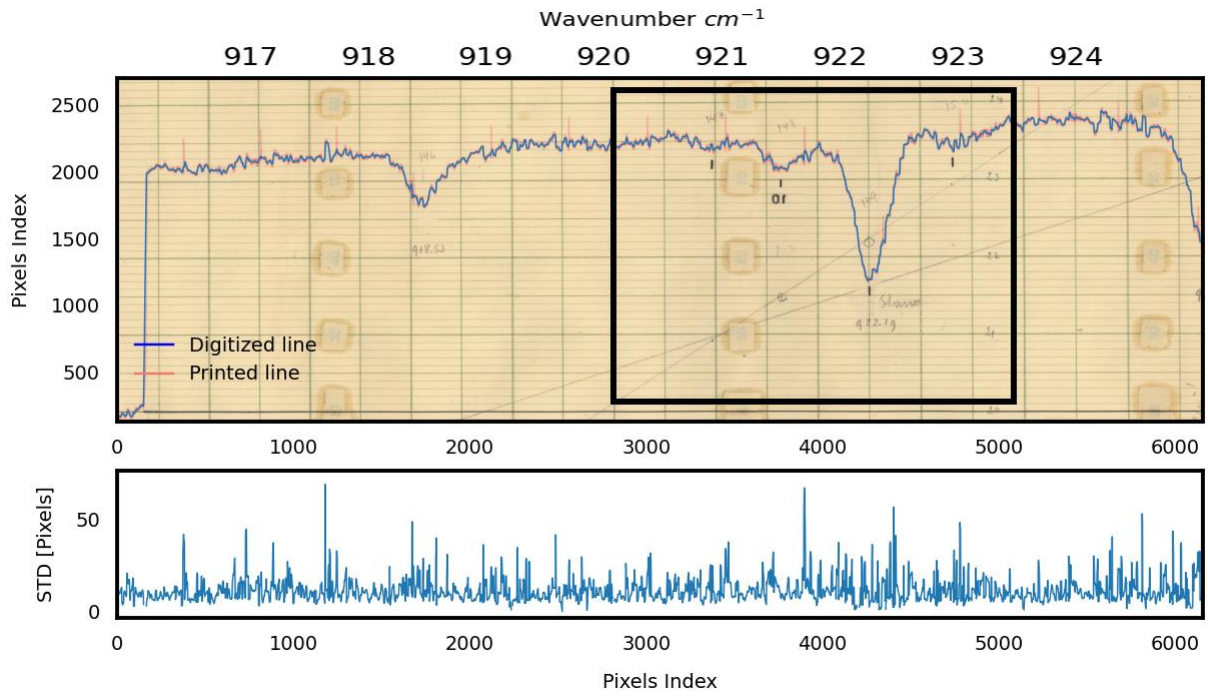


Figure 1: The original spectrum from which the CFC-12 surface value was retrieved. This spectrum was digitized and calibrated using the procedure described in Makkor et al (2024). The lower panel shows the standard digitization deviation of a 9.9 pixel average. The black rectangle shows the retrieval region used. 1

139 3.1.2 FTIR Measurements at Jungfrauoch

140 The first instrument (following the Pfund-type grating instruments at the same site) that
141 allowed routine measurements of atmospheric spectra at Jungfrauoch was a redesign of an
142 earlier Connes-type Fourier Transform Infrared (FTIR) spectrometer ([Zander et al., 2008](#)). By
143 changing from a step-scan mode to a continuous scan mode, the scan speed increased by 100-
144 fold. In addition to this, the instrument's optical length was doubled reaching a resolution of
145 0.0025 cm^{-1} . These changes allowed the start of recording atmospheric spectra regularly until
146 the instrument was retired in 2008. In the early 1990s, the University of Liège team deployed
147 and started to use a Bruker IFS 120HR instrument achieving a resolution of 0.001 cm^{-1} , and
148 recorded spectra alongside the home-made. This instrument was also decommissioned in 2024,
149 to be replaced with a Bruker IFS 125HR spectrometer.

150 3.1.3 Reconstructed histories of CFC-12 and AGAGE model

151 The first model-reconstructed histories of CFC-11 and CFC-12 were performed by [Walker et al.,](#)
152 [\(2000\)](#) from a two-box atmospheric model using estimates of annual atmospheric halocarbon
153 release, following the work of [Bullister & Weiss, \(1983\)](#). These estimates extend from 1935 to
154 1998 for CFC-12.

155 The 12-Box AGAGE model is a simplified advection-convection model developed by the AGAGE
156 group that uses emission estimates to calculate the atmospheric mole fractions of multiple
157 gases such as CFC-11, CFC-12 and others ([Rigby et al., 2013](#)). The emissions for this model have
158 been calculated up to the year 2024 using the approach provided by [Lickley et al., \(2020\)](#),
159 which employs the so-called Bayesian melding method developed by [Poole & Raftery, \(2000\)](#).
160 This technique enables the estimation of emissions by leveraging information from both
161 observed concentrations and the mechanistic simulation model of the bank, emissions, and
162 concentrations.

163 CFC-12 (as well as CFC-11) production data have been reported since 1975 by the CMA and the
164 Alternative Fluorocarbons Environmental Acceptability Study (AFEAS), covering most major
165 global producers. However, these reports exclude significant production from non-reporting
166 companies, particularly in the former Soviet Union and Eastern Europe. Emission estimates
167 incorporating these unreported sources were later provided by [Mccarthy et al., \(1977\)](#) who
168 estimated the total world annual production and subsequent world atmospheric emission from
169 1930 onwards.

170 4 Results

171 4.1 Estimation of CFC-12 level in 1951

172 The MW1 was used in the retrieval of CFC-12 from the digitized historical spectra (see [Figure 2](#)).
173 This microwindow is normally significantly influenced by water vapour, making it inappropriate
174 for ground-based retrievals at sea level but suitable for sites located at higher altitudes like
175 Jungfrauoch (3.58 km above sea level) where this influence is less critical. MW1 and MW2

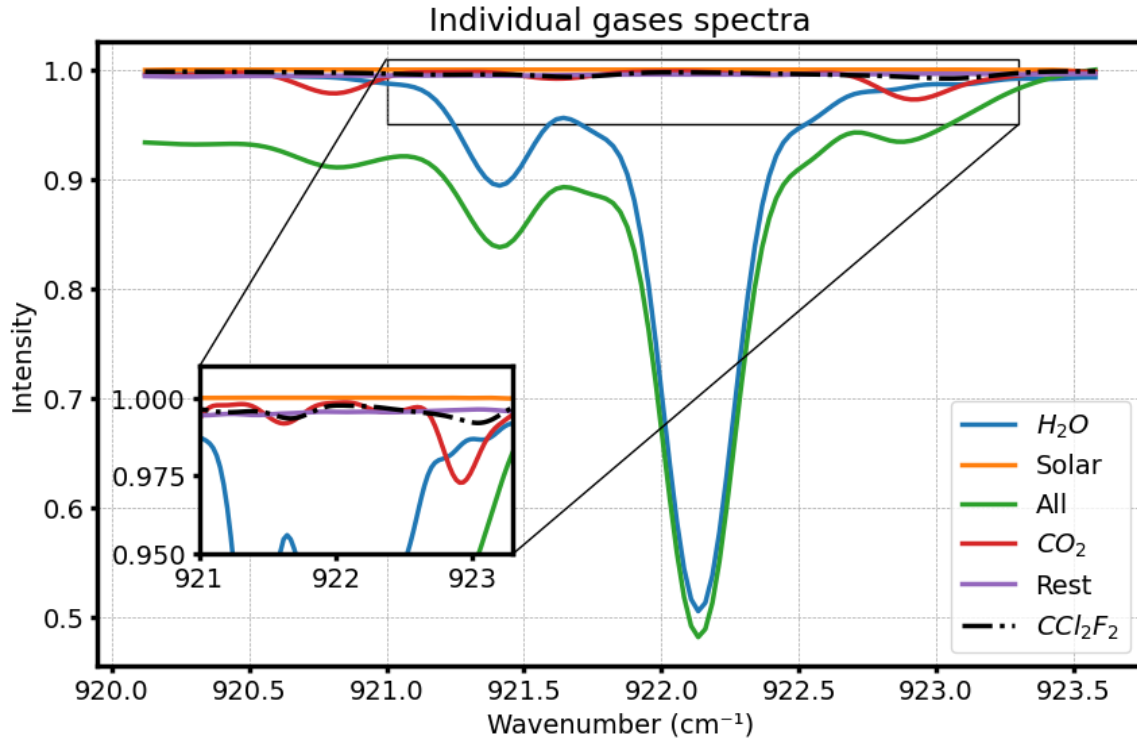
176 showed the best agreement and minimum intra-day variability in the total column values when
 177 adopting 300 and 65 for the Tikhonov regularization parameter, respectively. In MW1 the
 178 spectral bands of CO₂ and CFC-12 overlap, which requires a careful retrieval of CO₂ to get CFC-
 179 12 correct. The figure shows the measured and calculated spectra with a relatively good fit,
 180 albeit with high noise.

181 [Figure 3](#) shows all of the retrieved gases alongside CFC-12. The main contributions in this
 182 spectral interval come from H₂O and CO₂, but there is also a small and quantifiable contribution
 183 from CFC-12 in this spectrum (black dotted curve in [Figure 3](#)). This is not surprising since the
 184 production of CFC-12 started in the 1930s, and the compound was subsequently widely
 185 adopted by various industries as a foam agent and propellant. The early emissions of CFC-12
 186 mostly came from the United States and various European countries. The CFC-12 was detected
 187 in particular a the less noisy spectrum with an absorption strength slightly below 1%. The
 188 retrieval of CFC-12 from MW2 using the grating spectra was not possible due to significant
 189 influence from the noise.

190



191 *Figure 2: Fitting of the grating spectrum compared to the forward model calculated spectrum. This retrieval gives a CFC-
 192 12 surface value of 26.1 ppt. The lower panel shows the difference between the modeled and the observed spectrum. An
 optimal resolution of 0.277cm⁻¹ and a Triangular apodization were used.*



193

Figure 3: All the retrieved spectral lines from the old spectra. CFC-12 absorption although weaker is still present even on spectra from 1951 with an absorption strength of about 1%. The small zoomed-in window allows a closer look at the CFC-12 line (dotted black). The retrieval was performed using Tikhonov regularization facilitated by SFIT4 spectral fit routines.

194 4.2 Error Analysis

195 4.2.1 Error estimation of spectra from 1951

196 Quantifying the sources of errors in Pfund-type instrument from the 1950s involves considering
 197 two main categories of errors: those originating from the instrument itself and those arising
 198 from the paper spectra after processing (which includes digitization and calibration). One
 199 source of random error associated with the instrument, the zero transmission level offset,
 200 accounts for approximately 3% of the error (Zander et al., 1994). The resulting spectra have two
 201 error sources: a digitization error of around 1.55% and a wavenumber shift error of about 1%.
 202 The largest source of error comes from the retrieval itself. The total random error is about
 203 48.3% (retrieval, digitization and instrumental errors) and total systematic error of about 21.6%
 204 (see Table 1). The resolution of the historical spectra are not well known, but they are between
 205 0.1 and 0.4 cm^{-1} . Multiple retrievals were therefore performed for different resolutions. The
 206 resolution of 0.277 cm^{-1} , which has lowest calculated RMS was used in the retrieval.
 207 Additionally, the bias arising from the low resolution and triangular apodization when using the
 208 grating spectra was analysed. To achieve this, high-resolution FTIR spectra from the
 209 Jungfrauoch site were artificially lowered to resolutions of 0.1, 0.25 and 0.4 cm^{-1} (minimum,
 210 average and maximum resolutions) by truncating the Fourier transform of the high-resolution
 211 (HR) spectrum using the Bruker OPUS software (OPUS - Spectroscopy Software, n.d.).
 212 Subsequently, CFC-12 total columns were retrieved using these resolution values, then
 213 compared to the original values from the HR FTIR spectra. The triangular apodization was also
 214 applied to the lowered resolution FTIR spectra (See Table 2).

215

216 4.2.2 Error estimation of Jungfrauoch spectra

217 The largest source of error for the FTIR spectra is from temperature with a random and
 218 systematic error of 2.34% (in total). The random smoothing error $x_t - x_a$ is calculated from
 219 WACCM covariance matrix. The uncertainty coming from the solar zenith calculation is about
 220 0.1° for Jungfrauoch.

221

	Digitized 1951 grating spectrum	Bruker FTIR [1996 – present] spectra
	Random (%)	
Zero level offset	3.0	0.2
Temperature	0.72	1.34
Solar zenith angle	0.11	0.7
Phase function	-	0.28

Telluric species interference	35.6	0.02
Measurement	21.7	0.34
Digitization/Calibration	2.55	-
Total random	48.3	1.64
Systematic (%)		
Zero level offset	3	0.2
Spectroscopy (ATM19)	2.0	2
Temperature	4.8	1.0
Interfering species	21.5	-
Solar zenith angle	1.19	0.21
Phase function	-	0.28
Total systematic	21.6	2.31

222 *Table 1: Error summary of the retrieved CFC-12 values from the old 1951 grating data and the modern FTIR spectra.*

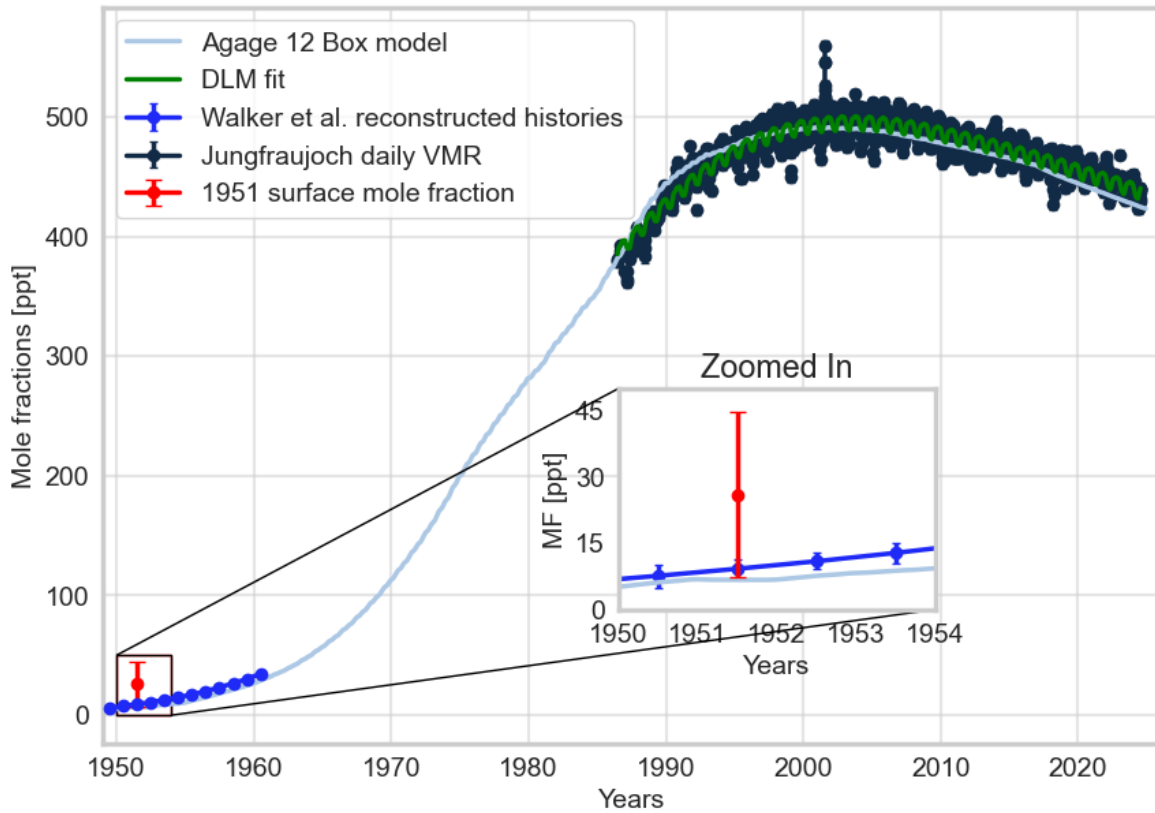
Resolution [cm ⁻¹]	0.1	0.25	0.4
Relative difference [%]	0.65	1.0	2.5

223 *Table 2: Relative difference in the retrieved CFC-12 value between the original high resolution FTIR spectra and the resolution-*
 224 *degraded ones.*

225 4.3 The full trend of CFC-12

226 [Figure 4](#) shows the long-term trend of CFC-12 from 1951 to present using various datasets and
 227 model results. The reconstructed historical model values represent the assumed CFC
 228 concentrations for the selected period between 1949 and 1960 (represented in the region of
 229 interest by the blue markers in [Figure 4](#)) from estimates of annual industrial production and
 230 emissions ([Walker et al., 2000](#)). The calculated CFC-12 concentration from these histories in
 231 1951 is 9.2 ± 0.2 ppt for the northern hemisphere. This reconstructed historical value have
 232 never be validated using actual measurements, because no measurements existed. The surface
 233 value we derived for 1951 of 26.1 ± 18.5 ppt from the spectra is 3 times larger than the
 234 reconstructed historical estimate for the northern hemisphere. These differences can be
 235 explained by inaccurate emissions in 1951, but the uncertainty of the measurement from the
 236 old instrument needs to also be considered. The concentration of CFC-12 from the old grating
 237 measurement was taken from the value given by the SFIT4 at the surface during the retrieval of
 238 the total column (which has a value of $3.36 \times 10^{14} \pm 1.58 \times 10^{14}$ molecule /cm²). The dry air mole

239 fractions from the FTIR measurements were also plotted and their trend fitted using a Dynamic
 240 Linear Model facilitated by the tool provided by [Hachmeister et al., \(2024\)](#). Additionally, the
 241 whole time series was complemented with the 12-Box AGAGE model with a CFC-12
 242 concentration value of 7.0 ± 0.28 ppt for 1951 to give a complete picture of the evolution of
 243 CFC-12 over the past decades and to account for the missing data between the 1950s and the
 244 start of FTIR measurements at Jungfraujoch.



245 *Figure 4: Atmospheric surface CFC-12 mole fraction (ppt) from 1951 to present. The measurement value in 1951 is*
 246 *retrieved in this work from solar measurements at Jungfraujoch in the same time period. It is compared to a 2-Box model*
 247 *reconstructed histories and 12-Box model from AGAGE. The retrieved mole fraction from FTIR measurements at*
Jungfraujoch are also represented and fitted using a Dynamic Linear Model (DLM).

248 5 Conclusions

249 A CFC-12 surface mole fraction of 26.1 ± 18.5 ppt for 1951 was derived from a grating
250 spectrometer at Jungfraujoch. Using results from a home-made FTIR-spectrometer (from 1984
251 to 2008) and from a commercial FTIR-spectrometer (from the beginning of the 1990s to
252 present), the interannual trend for the period 1951 – 2024 has been presented. The result for
253 1951 has been compared to estimates from reconstructed histories and AGAGE 12-Box models.
254 The estimated error value includes the preprocessing error (digitization and calibration) of the
255 historical paper spectra, error inherent to the instrument (finite S/N ratio) as well as the
256 retrieval error. The largest error source comes from the retrieval due to the weak signal-to-
257 noise ratio of the historical spectra.

258 The reconstructed histories and AGAGE 12-Box model estimates of CFC-12 for the northern
259 hemisphere in 1951 of about 9.2 ± 0.2 and 7.0 ± 0.28 ppt, respectively, are about 3 times lower
260 than the retrieved surface value from the historical grating instrument, but the error bars
261 overlap. We note, however, these values could be biased low due to erroneous emission
262 estimates in the 1950s.

263 The historical measurement has allowed us to retrieve the earliest atmospheric values of CFC-
264 12, predating previous earliest values by over two decades. The historical spectra also cover
265 other spectral regions, allowing the future retrieval of other trace gas concentrations in 1951.

266 Acknowledgments

- 267 • We gratefully acknowledge the Deutsche Forschungsgemeinschaft (DFG, German
268 Research Foundation) within the projects under the grant nos. 404/24-1 and PA 1714/8-
269 1.
- 270 • EM is a senior research associate with F.R.S. – FNRS (Brussels, Belgium). His 6-month
271 research stay at Universität Bremen was supported by a grant from the University of
272 Liège. The Belgian contribution was further supported by the Fonds de la Recherche
273 Scientifique (F.R.S. – FNRS, Brussels, Belgium; grant no. J.0126.21), the GAW-CH
274 program of MeteoSwiss (Zürich, CH) and the University of Liège. The ULiège team thanks
275 the International Foundation High Altitude Research Stations Jungfrauoch and
276 Gornergrat (HFSJG, Bern, CH) for supporting the facilities needed to perform the Fourier
277 transform infrared observations at Jungfrauoch.

278 Author contributions

279 JN and MPC supervised the work, MP provided the retrieval software and supervised the work,
280 MB and ZW edited the work. ZW provided advice on modelling. IPC and EM provided the CFC-
281 12 data retrieved from the Jungfrauoch FTIR spectra. JM retrieved the grating spectra, ran the
282 models/comparisons and authored the letter. All co-authors provided comments and
283 suggestions.

284

285 Availability and data statement

286 The FTIR measurements are regularly provided and updated by the GIRPAS team and can be
287 freely downloaded from [https://www-
288 air.larc.nasa.gov/pub/NDACC/PUBLIC/stations/jungfrauoch/hdf/ftir/](https://www-air.larc.nasa.gov/pub/NDACC/PUBLIC/stations/jungfrauoch/hdf/ftir/) (last accessed
289 11/06/2025)

290 The digitized grating spectra can be freely downloaded under
291 <https://zenodo.org/records/14537672> (last accessed 11/06/2025)

292 SFIT4 retrieval program and related tools can be freely downloaded under
293 <https://wiki.ucar.edu/spaces/sfit4/pages/402424651/SFIT4+Version+1.0.xx+Release> (last
294 accessed 11/06/2025)

295 **References**

- 296 Bullister, J. L., & Weiss, R. F. (1983). Anthropogenic Chlorofluoromethanes in the Greenland and Norwegian
297 Seas. *Science*, 221(4607), 265–268. <https://doi.org/10.1126/science.221.4607.265>
- 298 Cantos, I. P., Mahieu, E., Chipperfield, M. P., Smale, D., Hannigan, J. W., Friedrich, M., et al. (2022).
299 Determination and analysis of time series of CFC-11 (CCl₃F) from FTIR solar spectra, in situ observations, and
300 model data in the past 20 years above Jungfraujoch (46°N), Lauder (45°S), and Cape Grim (40°S) stations.
301 *Environmental Science: Atmospheres*, 2(6), 1487–1501. <https://doi.org/10.1039/D2EA00060A>
- 302 CMA. (1980). 1980 world production and sales of fluorocarbons FC-11 and FC-12 (1981). Chemical
303 Manufacturers Association.
- 304 Cunnold, D., Alyea, F., & Prinn, R. (1978). A methodology for determining the atmospheric lifetime of
305 fluorocarbons. *Journal of Geophysical Research: Oceans*, 83(C11), 5493–5500.
306 <https://doi.org/10.1029/JC083iC11p05493>
- 307 Engel, A., Schmidt, U., & McKenna, D. (1998). Stratospheric trends of CFC-12 over the past two decades: Recent
308 observational evidence of declining growth rates. *Geophysical Research Letters*, 25(17), 3319–3322.
309 <https://doi.org/10.1029/98GL02520>
- 310 Griffiths, P. R. (2006). Resolution and Instrument Line Shape Function. In *Handbook of Vibrational Spectroscopy*.
311 John Wiley & Sons, Ltd. <https://doi.org/10.1002/0470027320.s0111>
- 312 Hachmeister, J., Schneising, O., Buchwitz, M., Burrows, J. P., Notholt, J., & Buschmann, M. (2024). Zonal
313 variability of methane trends derived from satellite data. *Atmospheric Chemistry and Physics*, 24(1), 577–595.
314 <https://doi.org/10.5194/acp-24-577-2024>
- 315 Kalnay, E., Kanamitsu, M., Kistler, R., Collins, W., Deaven, D., Gandin, L., et al. (1996). The NCEP/NCAR 40-
316 Year Reanalysis Project. *Bulletin of the American Meteorological Society*, 77(3), 437–472.
317 [https://doi.org/10.1175/1520-0477\(1996\)077<0437:TNYRP>2.0.CO;2](https://doi.org/10.1175/1520-0477(1996)077<0437:TNYRP>2.0.CO;2)
- 318 Lickley, M., Solomon, S., Fletcher, S., Velders, G. J. M., Daniel, J., Rigby, M., et al. (2020). Quantifying
319 contributions of chlorofluorocarbon banks to emissions and impacts on the ozone layer and climate. *Nature*
320 *Communications*, 11(1), 1380. <https://doi.org/10.1038/s41467-020-15162-7>
- 321 Lovelock, J. E. (1971). Atmospheric Fluorine Compounds as Indicators of Air Movements. *Nature*, 230(5293),
322 379–379. <https://doi.org/10.1038/230379a0>

- 323 Mahieu, E., Duchatelet, P., Demoulin, P., Walker, K. A., Dupuy, E., Froidevaux, L., et al. (2008). Validation of
324 ACE-FTS v2.2 measurements of HCl, HF, CCl₃F and CCl₂F₂ using space-, balloon- and ground-based instrument
325 observations. *Atmospheric Chemistry and Physics*, 8(20), 6199–6221. <https://doi.org/10.5194/acp-8-6199-2008>
- 326 Makkor, J., Palm, M., Buschmann, M., Mahieu, E., Chipperfield, M. P., & Notholt, J. (2024). Digitization and
327 calibration of historical solar absorption infrared spectra from the Jungfrauoch site. *Atmospheric Measurement*
328 *Techniques*, 1–15. <https://doi.org/https://doi.org/10.5194/amt-18-1105-2025>
- 329 Mccarthy, R. L., Bower, F. A., & Jesson, J. P. (1977). The fluorocarbon-ozone theory—I. Production and release—
330 world production and release of CCl₃F and CCl₂F₂ (fluorocarbons 11 and 12) through 1975. *Atmospheric*
331 *Environment* (1967), 11(6), 491–497. [https://doi.org/10.1016/0004-6981\(77\)90065-8](https://doi.org/10.1016/0004-6981(77)90065-8)
- 332 Midgley, T. Jr., & Henne, A. L. (1930). Organic Fluorides as Refrigerants. *Industrial & Engineering Chemistry*,
333 22(5), 542–545. <https://doi.org/10.1021/ie50245a031>
- 334 Migeotte, M. (1949). The Fundamental Band of Carbon Monoxide at 4.7 μ in the Solar Spectrum. *Physical Review*,
335 75(7), 1108–1109. <https://doi.org/10.1103/PhysRev.75.1108>
- 336 Migeotte, M., Neven, L., & Swensson, J. (1956). THE SOLAR SPECTRUM FROM 2.8 TO 23.7 MICRONS.
337 PART I. PHOTOMETRIC. Retrieved from [https://www.semanticscholar.org/paper/THE-SOLAR-SPECTRUM-](https://www.semanticscholar.org/paper/THE-SOLAR-SPECTRUM-FROM-2.8-TO-23.7-MICRONS.-PART-Migeotte-Neven/e708a03953f7ce76c2d78aac832e05214c7d8357)
338 [FROM-2.8-TO-23.7-MICRONS.-PART-Migeotte-Neven/e708a03953f7ce76c2d78aac832e05214c7d8357](https://www.semanticscholar.org/paper/THE-SOLAR-SPECTRUM-FROM-2.8-TO-23.7-MICRONS.-PART-Migeotte-Neven/e708a03953f7ce76c2d78aac832e05214c7d8357)
- 339 Molina, M. J., & Rowland, F. S. (1974). Stratospheric sink for chlorofluoromethanes: Chlorine atomc-atalsed
340 destruction of ozone. *Nature*, 249(5460), 810–812. <https://doi.org/10.1038/249810A0>
- 341 Montzka, S. A., Dutton, G. S., Yu, P., Ray, E., Portmann, R. W., Daniel, J. S., et al. (2018). An unexpected and
342 persistent increase in global emissions of ozone-depleting CFC-11. *Nature*, 557(7705), 413–417.
343 <https://doi.org/10.1038/s41586-018-0106-2>
- 344 Montzka, S. A., Dutton, G. S., Portmann, R. W., Chipperfield, M. P., Davis, S., Feng, W., et al. (2021). A decline
345 in global CFC-11 emissions during 2018–2019. *Nature*, 590(7846), 428–432. [https://doi.org/10.1038/s41586-021-](https://doi.org/10.1038/s41586-021-03260-5)
346 [03260-5](https://doi.org/10.1038/s41586-021-03260-5)
- 347 OPUS - Spectroscopy Software. (n.d.). Retrieved July 26, 2024, from [https://www.bruker.com/en/products-and-](https://www.bruker.com/en/products-and-solutions/infrared-and-raman/opus-spectroscopy-software.html)
348 [solutions/infrared-and-raman/opus-spectroscopy-software.html](https://www.bruker.com/en/products-and-solutions/infrared-and-raman/opus-spectroscopy-software.html)
- 349 Poole, D., & Raftery, A. E. (2000). Inference for Deterministic Simulation Models: The Bayesian Melding
350 Approach. *Journal of the American Statistical Association*, 95(452), 1244–1255.

351 <https://doi.org/10.1080/01621459.2000.10474324>

352 Rigby, M., Prinn, R. G., O'Doherty, S., Montzka, S. A., McCulloch, A., Harth, C. M., et al. (2013). Re-evaluation
353 of the lifetimes of the major CFCs and CH₃CCl₃ using atmospheric trends. *Atmospheric Chemistry and Physics*,
354 13(5), 2691–2702. <https://doi.org/10.5194/acp-13-2691-2013>

355 Rodgers, C. D. (2000). *Inverse Methods for Atmospheric Sounding: Theory and Practice*.
356 <https://doi.org/10.1142/3171>

357 Scientific Assessment of Ozone Depletion 2022: Executive Summary. (2022). Retrieved November 15, 2023, from
358 <https://csl.noaa.gov/assessments/ozone/2022/executivesummary/>

359 The Kigali Amendment. (2016). Retrieved January 22, 2025, from [https://ozone.unep.org/treaties/montreal-](https://ozone.unep.org/treaties/montreal-protocol/amendments/kigali-amendment-2016-amendment-montreal-protocol-agreed)
360 [protocol/amendments/kigali-amendment-2016-amendment-montreal-protocol-agreed](https://ozone.unep.org/treaties/montreal-protocol/amendments/kigali-amendment-2016-amendment-montreal-protocol-agreed)

361 United Nations Treaty Collection. (1989). Retrieved November 15, 2023, from
362 https://treaties.un.org/pages/ViewDetails.aspx?src=TREATY&mtdsg_no=XXVII-2-a&chapter=27&clang=_en

363 Walker, S. J., Weiss, R. F., & Salameh, P. K. (2000). Reconstructed histories of the annual mean atmospheric mole
364 fractions for the halocarbons CFC-11, CFC-12, CFC-113, and carbon tetrachloride. *Journal of Geophysical*
365 *Research: Oceans*, 105(C6), 14285–14296. <https://doi.org/10.1029/1999JC900273>

366 Zander, R., Ehhalt, D. H., Rinsland, C. P., Schmidt, U., Mahieu, E., Rudolph, J., et al. (1994). Secular trend and
367 seasonal variability of the column abundance of NeO above the Jungfraujoch station determined from IR solar
368 spectra. *JOURNAL OF GEOPHYSICAL RESEARCH*, 99(D8), 745–761. <https://doi.org/10.1029/94JD01030>

369 Zander, R., Mahieu, E., Demoulin, P., Duchatelet, P., Roland, G., Servais, C., et al. (2008). Our changing
370 atmosphere: Evidence based on long-term infrared solar observations at the Jungfraujoch since 1950. *Science of The*
371 *Total Environment*, 391(2–3), 184–195. <https://doi.org/10.1016/J.SCITOTENV.2007.10.018>

372